Self-organization of yeast cells on modified polymer surfaces after dewetting: new perspectives in cellular patterning

2006 J. Phys.: Condens. Matter 18 S2221

(http://iopscience.iop.org/0953-8984/18/33/S36)

INSTITUTE OF PHYSICS PUBLISHING JOURNAL OF PHYSICS: CONDENSED MATTER

J. Phys.: Condens. Matter **18** (2006) S2221–S2230 doi:10.1088/0953-8984/18/33/S36

Self-organization of yeast cells on modified polymer surfaces after dewetting: new perspectives in cellular patterning

S Carnazza[1], S Satriano[2] and S Guglielmino[1]

[1] Department of Microbiological, Genetic and Molecular Sciences, University of Messina, Messina, Italy
[2] Department of Chemical Sciences, University of Catania, Catania, Italy

E-mail: santina.carnazza@unime.it

Received 16 January 2006, in final form 28 June 2006
Published 4 August 2006
Online at stacks.iop.org/JPhysCM/18/S2221

Abstract

In recent years, biological micro-electro-mechanical systems (commonly referred to as BioMEMS) have found widespread use, becoming increasingly prevalent in diagnostics and therapeutics. Cell-based sensors are nowadays gaining increasing attention, due to cellular built-in natural selectivity and physiologically relevant response to biologically active chemicals. On the other hand, surrogate microbial systems, including yeast models, have become a useful alternative to animal and mammalian cell systems for high-throughput screening for the identification of new pharmacological agents. A main obstacle in biosensor device fabrication is the need for localized geometric confinement of cells, without losing cell viability and sensing capability. Here we illustrate a new approach for cellular patterning using dewetting processes to control cell adhesion and spatial confinement on modified surfaces. By the control of simple system parameters, a rich variety of morphologies, ranging through hexagonal arrays, polygonal networks, bicontinuous structures, and elongated fingers, can be obtained.

1. Introduction

In recent years, the biological and biomedical applications of micro- and nanotechnology have become increasingly prevalent, and biological micro-electro-mechanical systems (BioMEMS) have found widespread use in a wide variety of applications that encompass all interfaces of biology and biomedical sciences with micro- and nanoscale systems. Diagnostics represents the largest and most researched BioMEMS area. Within the last few years, many BioMEMS devices for diagnostic applications, termed Biochips, have been developed for sensitive, rapid and real-time measurements.

In particular, biosensors have recently generated substantial interest. They are analytical devices that combine a biologically sensitive element (bio-receptor) with a physical or chemical transducer to selectively and quantitatively detect the presence of specific compounds in a given external environment. There is currently a wide interest in using whole cells as functional components in biosensors for their built-in natural selectivity to biologically active chemicals and the physiologically relevant response that can be monitored by measuring products of reporter genes. These devices find widespread use in detection of toxic compounds and pathogens in the environment as well as in high-throughput screening (HTS) for new drug discovery. Cell-based assays have significant advantages over *in vitro* assays. First, the starting material (the cell) self-replicates, avoiding the investment involved in preparing a purified target, in chemically modifying the target and so on. Second, the targets and readouts are examined in a biological context that more faithfully mimics the normal physiological situation. Third, cell-based assays can provide insights into bio-availability and cytotoxicity.

However, mammalian cells are expensive to culture and difficult to propagate in the automated systems used for HTS; an alternative to mammalian cell-based assays is to reproduce the desired human physiological process in a micro-organism such as yeast [1]. It is relatively easy to transfect yeast with human DNA encoding receptors or other components of signal transduction pathways, and this fact has been used to develop a HTS screening system [2]. The signalling pathways in yeast and humans are sufficiently related to permit functional evaluation of human receptors in yeast cells [3]. Because of the straightforward manipulation of genetic information in yeast, it is relatively simple to generate a family of strains that differ by a single human gene, to facilitate the analysis of screening data [4].

The ease and low cost of growing yeasts, their ready genetic manipulation, and their resistance to solvents make yeast an attractive option for cell-based HTS.

The main trends in the BioMEMS research are miniaturization and integration of components and the use of microtechniques to improve immobilization and spatial confinement methods. These and other applications requiring the cell/surface interaction account for considerable efforts in development of surface modification and cellular patterning methods, that are very important tools for fundamental studies in biology, especially on single cells, as well as for preparation of chip-based systems in biotechnology.

One of the crucial features in the fabrication of effective cell-based biosensors is the development of immobilization technologies for tethering biological systems to surfaces in selected device areas, in proximity to the transducer surface. The ability to generate even large area patterns of biological materials offers great advantages and opens the door to a wide range of applications in the field of biosensor technology and drug discovery.

A number of methods have been reported for patterning cells, but it is nowadays difficult to obtain pre-casting cell arrays with good fidelity and without losing cell viability and sensing activity.

Recently, Lee *et al* [5] have presented an alternative approach for controlled two-dimensional nanoparticle organization on a solid substrate by applying dewetting patterns of charged polymer solutions as a templating system. Because the template morphology depends on easily controlled parameters, such as the polymer charge density, concentration and dewetting rate, as previously demonstrated by the same authors [6], this method of controlled particle alignment held an attractive feature in its relative simplicity, compared to other methods that require chemical modifications and ligand grafting onto the particles and on the templating substrate.

Thus, complex morphologies including holes, polygonal networks, bicontinuous structures and elongated structures that are stabilized by viscous forces were produced from dewetting and served as potential templates for nanoparticle organization on a solid substrate. The particle

ordering process was a two-step mechanism: an initial confinement of the nanoparticles in the dewetting structures and self-assembly of the particles within these structures upon further drying by lateral capillary attractions [6], as firstly described for micrometre-size polystyrene latex spheres dewetted on a glass substrate [7].

The dewetting of charged polymer solutions was shown to be a potential method for controlled nanoparticle assembly on a solid substrate. While dewetting morphologies were controlled by polymer solution properties, the templating of the nanoparticle assembly by these polymer films was controlled by the particle size with respect to the thickness of the dewetting film. The easy control of these parameters renders this approach highly attractive as a potential method for directed nanoparticle organization.

In this paper, we investigate the possibility to control yeast cell organization on polymer surfaces to produce open structures, such as polygonal networks and bicontinuous or elongated structures, using dewetting patterns as templates. The basic idea is to obtain a cellular self-assembly on chemically well defined solid substrates after controlled dewetting processes.

When an aqueous dispersion of particles is deposited on freshly cleaved mica and allowed to dry by evaporation, regions of two-dimensional aggregates are formed, resulting from the self-assembly of particles, a process that has been described by the two-stage mechanism [7]: formation of a nucleus of an ordered phase and convective transport of particles toward the ordered domain. Thus, to form open structures from a drying cell suspension, a control over the nucleation stage of the ordering process is required. The approach adopted in the present study involves the control of the nucleation process, by initial cell–substrate interactions, depending on both cell and polymer surface properties. Lateral capillary attractions of the cells confined in the dewetting structures will further complete the self-organization process. With this aim, chemically well defined polymer surfaces were prepared and characterized to be used in cell adhesion and distribution investigation; adhesion of the yeast *Candida albicans* on the obtained substrates was investigated; then, the possibility of a selective cellular patterning by means of self-organization phenomena prompted by dewetting processes was evaluated.

2. Experimental details

2.1. Substrate preparation and characterization

Poly(hydroxymethylsiloxane) (PHMS, Honeywell, US) and poly(ethyleneterephthalate) (PET, Aldrich) thin films (thickness of 500 $\pm$ 15 nm) were spin-coated onto the polished side of monocrystalline silicon (100). The PHMS- and PET-coated wafers were cut into pieces of area 1×0.5 cm^2. The samples have been successively modified by O_2 plasma treatments and by 50 keV Ar^+ beams, in order to change the wettability of surfaces [8]. Polystyrene of Petri dishes was used as a reference hydrophobic substrate.

Oxygen plasma treatments were carried out in a March Instrument solid-state Plasmod unit (Concord, CA, USA) supplied with an RF generator with an excitation frequency of 13.56 MHz. The plasma treatments were carried out for 1 min at a power of 100 W and pressure 66.6 Pa, then the samples were copiously washed with Millipore water and rinsed under nitrogen blow.

Ion irradiation treatments were performed at room temperature by means of a Danfysik ion implanter using 50 keV Ar^+ ions. The ion dose was controlled with a Faraday cup and set at a fluence of 1×10^{15} ions cm^{-2}, with a current density of 1.5 μA cm^{-2}. The beam was rastered over the samples in order to keep the thermal load as low as possible.

The physico-chemical characterization of the substrate surfaces before and after the modification steps was performed by means of static and dynamic water contact angle (WCA) measurements and atomic force microscopy (AFM).

Measurements of water contact angle were performed on a half automatic video-based OCA30 instrument (Dataphysics) at 25 °C and 45% relative humidity. The static water contact angles (WCA_{static}) were measured by using the sessile drop method. Liquid drops of 2 μl were applied on at least five different regions of each sample surface and both sides of the two-dimensional projection of the droplets were analysed by digital image analysis.

The water advancing and receding contact angles (WCA_{adv} and WCA_{rec}, respectively) were measured by the needle–syringe method [9].

The micro- and nanomorphology of the surfaces was measured with a Multimode/Nanoscope IIIA atomic force microscope (AFM, Veeco) in tapping mode in air with a standard silicon tip. Data were acquired on at least three square frames having edges of 10 μm, 1 μm, and 300 nm, with 512 $\times$ 512 data points and a scan rate of 1.989 Hz. Images were recorded using both height and phase-shift channels.

2.2. Cell adhesion assay

Candida albicans (ATCC 10231) was used throughout all experiments. It was grown in tryptone soya broth (TSB, Liofilchem, Teramo, Italy) with shaking at 30 °C. An overnight TSB culture was diluted 1:100 in fresh TSB and incubated with shaking at 30 °C for 6 h, at which time cells had been previously verified to be in midexponential phase. Cells were harvested by centrifugation, washed twice (0.01 M PBS pH 7.4), and diluted in 0.01 M PBS pH 7.4 to an optical density of 1.0 at 400 nm (Beckman DU640 spectrophotometer) corresponding to approximately 3×10^7 viable cells (CFU) per millilitre. Previous studies had demonstrated that this optical density corresponds to the maximal adhesion in the experimental conditions adopted here. As the aim of this paper was to deal not with the mere number of adhering yeast cells but rather with the two-dimensional cellular organization on the modified polymer surfaces, we have used a stagnation point flow chamber according to the methods previously described [10]. The deposition was allowed to occur at 30 °C for 2 h, then visualization of cells adhering to the surfaces was obtained by a modification of Ramsay's [11] acridine orange staining procedure. Briefly, a stock solution of acridine orange (300 μg ml^{-1} in 0.01 M PBS, pH 8.2, with 0.01% merthiolate) was injected into the chamber and samples were directly observed by a Leica DMRE epifluorescence microscope endowed with motor focus controlled by Leica Fluo-Software.

A quantitative evaluation of cells adhering onto the different materials was performed using the Scion Image software (Windows version of NIH Image software), in terms of integrated density (I.D. $= N \times (M - B)$, where N is the number of pixels in the selection, M is the average grey value of the pixels, and B is the most common pixel value) [10].

2.3. Cellular patterning by dewetting

The dewetting effects in cell patterning were monitored by using a cell suspension (0.01 M PBS at pH 7.4) with a concentration of approximately 3×10^7 cells ml^{-1}. Such a cell suspension was transferred to a Petri dish containing the small pieces of plasma-treated and Ar^+-irradiated PHMS and PET samples. The yeast cells were allowed to adhere onto the polymers for 2 h, then the unattached cells were removed by dipping the samples twice in PBS and twice in sterile ultra-pure water. The adhered cells were dried in air and then stained with acridine orange as described above.

Samples were observed by a Leica DMRE epifluorescence microscope. In order to visualize the extent of cellular distribution on polymer surfaces, microscopic observations at 400$\times$ magnification were performed on the whole surface of each sample, and the single optical fields were acquired by a Leica DC300F Camera and Leica Qwin software.

Table 1. Static and dynamic water contact angle (WCA) values onto the various surfaces.

Sample	Static WCA (deg)[a]	Advancing WCA (deg)[a]	Receding WCA (deg)[a]	Hysteresis (deg)
Untreated PHMS	88.0 ± 1.1	96.8 ± 1.7	62.4 ± 2.0	34.4
Plasma-treated PHMS	17.5 ± 2.2	25.9 ± 3.2	11.4 ± 0.8	14.5
Ar^+-irradiated PHMS	37.6 ± 0.6	41.4 ± 0.9	21.5 ± 2.1	19.9
Untreated PET	73.2 ± 0.2	75.9 ± 1.4	56.0 ± 1.1	19.9
Plasma-treated PET	52.6 ± 2.9	67.0 ± 2.8	21.0 ± 1.4	46.0
Ar^+-irradiated PET	74.5 ± 1.7	74.3 ± 1.8	54.3 ± 1.5	31.9
Polystyrene	81.4 ± 3.2	102.6 ± 2.5	81.4 ± 1.9	21.3

[a] Mean values from five independent measurements for each surface are shown.

3. Results and discussion

3.1. Substrate characterization

The water wettability properties of the various investigated surfaces are reported in table 1, in terms of both static and dynamic water contact angles (WCAs).

The very hydrophobic PHMS surfaces became moderately hydrophilic after ion irradiation and very hydrophilic after plasma treatment. The contact angle hysteresis, i.e. the difference between WCA_{adv} and WCA_{rec}, exhibits a decrease parallel to the increase of the hydrophilic character after ion irradiation and plasma treatment, respectively. This fact suggests that the surface-modified PHMS surfaces do not undergo significant changes of roughness or of the extension of chemically heterogeneous micro-domains. According to this observation, we briefly recall previous results from this laboratory, which showed that both plasma and ion irradiation of PHMS induce a mild smoothing of the surfaces (with root mean squared roughness values R_q in the range of 0.2–0.5 nm), and that both types of surface modification promote the formation of homogeneous $SiO_{x-\varepsilon}C_{\varepsilon}$ phases [8, 10, 12].

As to the PET samples, table 1 shows that the water wettability of PET slightly decreases after Ar^+ irradiation, and significantly increases after O_2 plasma treatment. The observed trend of hysteresis in this case is very different from that observed for PHMS samples. In fact, for both Ar^+-irradiated and plasma-treated PET the WCA hysteresis noticeably increases, suggesting either a roughness increase and/or the formation of chemically heterogeneous domains. Again, one should recall that AFM analysis of these samples indicated a negligible change of surface roughness ($R_q \sim$ 0.2–0.4 nm), while the XPS data revealed that Ar^+ irradiation and O_2 plasma treatment of PET, producing respectively the loss and the increase of oxygen content at surfaces, induce the formation of amorphous carbon phases containing strikingly different amounts of linked oxygen [8, 10, 12, 13].

The above described results indicated that the two different polymers must be discussed separately due to the striking differences in the relative chemical homogeneity and in the whole chemical structure of the surfaces [8, 10, 12, 13]. More particularly, focusing the attention at the wettability of the surfaces, the PHMS surfaces employed in the present work are good models to follow the gradual transition from hydrophobic to highly hydrophilic surface character, while the PET surfaces exhibit a moderate and stable hydrophobic character, irrespective of the irradiation treatments.

3.2. Cell adhesion assay

A very poor adhesion was observed for untreated PHMS and PET, similar to that found for the reference polystyrene surface, while adhesion was improved on modified substrates, with the highest number of adhering cells on both Ar^+-irradiated polymer surfaces (figure 1).

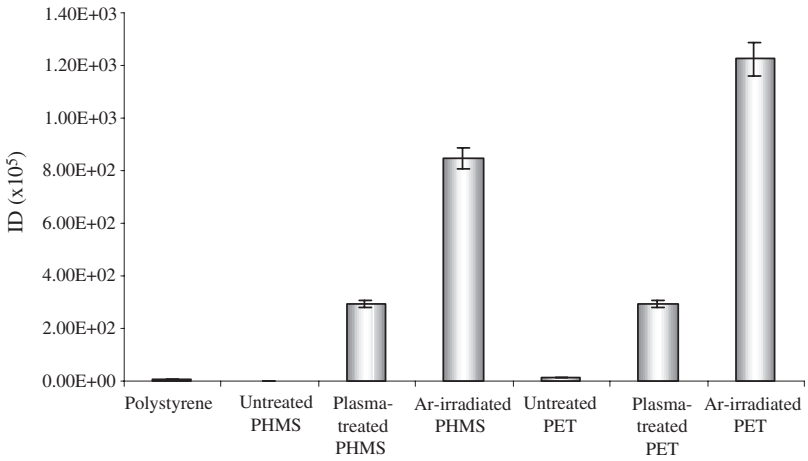

Figure 1. Extents of adhesion of *C. albicans* cells to the different chemically modified substrates, as compared to the untreated PHMS and PET and the reference polystyrene surface, in terms of I.D. mean values. Errors bars indicate standard deviations.

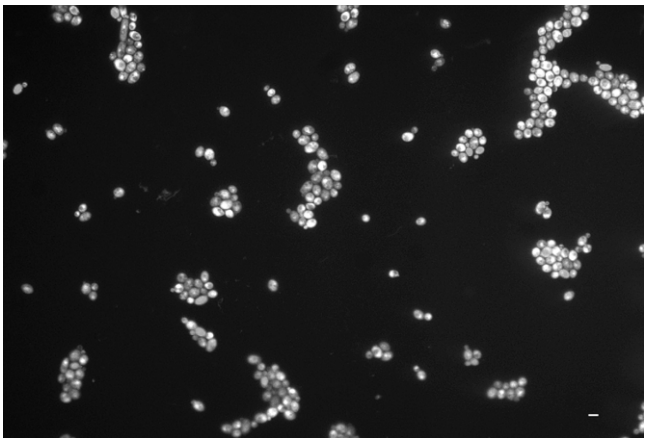

Figure 2. Fluorescence microscopy of *C. albicans* cells adhering on plasma-treated PET. Bar: 10 μm.

3.3. Cellular patterning by dewetting

Plasma-treated and Ar^+-irradiated PHMS and PET surfaces were used in assays of cellular patterning by dewetting, as they supported the best adhesion of *C. albicans* cells.

The reported results showed that a rich variety of morphologies of cell distribution, ranging through holes, polygonal networks, bicontinuous structures, droplets, hexagonal arrays and cylindrical structures, are those typical of dewetting processes reported in the literature for thin polymeric films or nanoparticles [5–7].

Indeed, it seems apparent that self-organization of yeast cells on the various studied surfaces in the present work may lead to a variety of different structures going from droplets (figure 2) and long cylindrical chains (figure 3) to bicontinuous structures (figure 4) and open polygonal networks (figure 5).

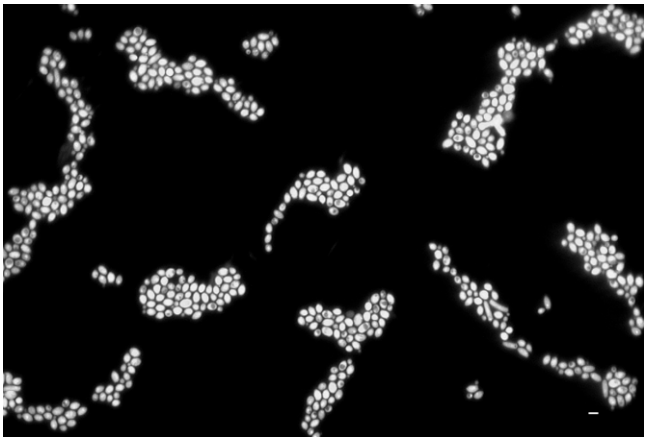

Figure 3. Fluorescence microscopy of *C. albicans* cells adhering on plasma-treated PHMS. Bar: 10 μm.

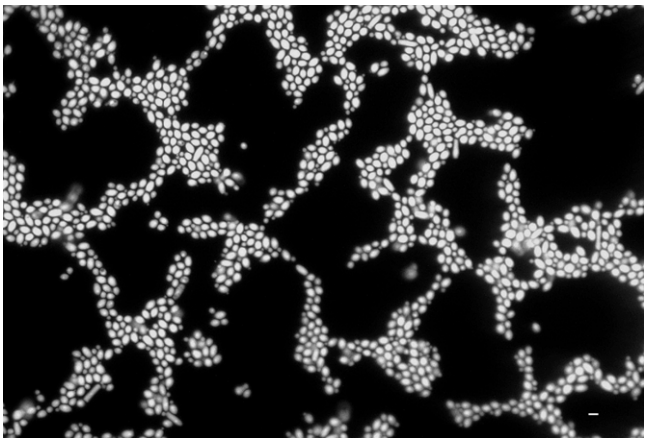

Figure 4. Fluorescence microscopy of *C. albicans* cells adhering on Ar^+-irradiated PHMS. Bar: 10 μm.

It is worth noting that in the obtained dewetting structures a typical hexagonal array can be often observed (figure 6), similar to that produced by more laborious and expensive micropatterning techniques [14].

Furthermore, the obtained structures are unusually stable and resist fragmentation, likely due to the predominant viscous forces that counter capillary forces responsible for fragmentation.

These different structures can be accounted for in terms of the different wettability properties of PHMS and PET. In fact, the well separated structures observed for plasma-treated PHMS can be understood in terms of relatively high hydrophilicity of these substrates, while the aggregation observed for Ar^+-irradiated PHMS seems to reflect the relative hydrophobicity of these surfaces. Similarly, in the case of plasma-treated and Ar^+-irradiated PET surfaces, the transition from separated structures to bicontinuous structures is observed, parallel to the decrease of water wettability from plasma-treated to Ar-irradiated samples.

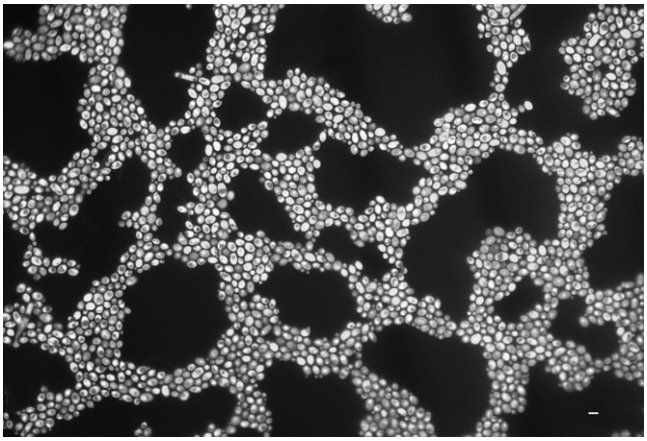

Figure 5. Fluorescence microscopy of *C. albicans* cells adhering on Ar^+-irradiated PET. Bar: 10 μm.

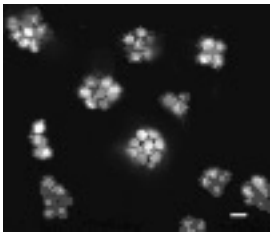

Figure 6. Fluorescence microscopy of *C. albicans* cells adhering on plasma-treated PET. Hexagonal arrays of yeast cell aggregates are visible. Bar: 10 μm.

In addition, for both PHMS and PET samples, the observation of isolated cellular aggregates, in the case of plasma-treated surfaces, and bicontinuous cellular patterns, for the Ar^+-irradiated surfaces, is well in accordance with the trends of receding contact angle values for the two polymers (see table 1), which indeed are representative of the dewetting behaviour of a water droplet on the investigated surfaces. In fact, for both PHMS and PET surfaces the WCA_{rec} values for plasma-treated surfaces are about half of the corresponding values for the ion-irradiated ones. It remains to explain the similarity between such different surfaces as Ar^+-irradiated PHMS and PET, which have indeed significantly different contact angles and hysteresis behaviour (see table 1).

As to the whole dewetting process, a two-step mechanism, consisting of an initial confinement of yeast cells in the dewetting structure and self-assembly of the confined cells upon further drying by lateral capillary attractions, is likely also involved in the self-organization process observed in our study. In fact, when the cell suspension is incubated on the modified polymer surfaces and then allowed to dry by evaporation of liquid phase, two-dimensional cellular aggregates are formed, in a way similar to that described for inert particles [7]. Once ordered regions are formed, the thinning of the water layer inside them is slowed due to the hydrophilicity of the cells. The evaporation from the concave menisci between cells, clustered in a nucleus, increases the local curvature and hence the local sucking capillary pressure. This brings about an intensive water influx from the thicker parts of the layer where the pressure is higher. The convective influx carries along the suspended cells toward the

clusters, where they remain attached, pressed by the hydrodynamic pressure of the water and captured by the capillary attraction.

Both surface chemical structure and topography can affect the water structuring near surface, which in turn determines capillary forces responsible for the formation of ordered clusters in the first stage of the self-assembly process. We have operated on this first step of cellular self-organization, just by tailoring the physico-chemical surface properties of polymeric substrates. By controlling the number of cells and time periods of incubation on substrates, we have been able to operate on the second step of cellular self-organization prompted by dewetting, affecting convective forces depending on menisci between cells clustered in ordered nuclei.

4. Conclusion

In the present paper we give the first demonstration of self-organization of microbial cells after dewetting on modified polymer substrates. A potential micropatterning method, simpler and more rapid than the usual ones, but reliable and controlled by well defined parameters, is proposed.

Our method offers several advantages over traditional cellular patterning methods. We utilize a method yielding excellent spatial control, to shape and confine our biologically sensitive layer in a pre-casting platform array for potential whole-cell biosensors. We have demonstrated the formation of geometrically well defined cellular patterns. Single yeast cells were immobilized, forming a high-density fractal array that allows for a scale-free measurement of cell response by a potential transducer. This whole-cell biosensor platform should be very sensitive since each cell acts as an individual, independent sensor, and averaging responses from multiple identical sensors improves the signal to noise ratio. The cellular patterning procedure is simple and the immobilized cells retain their full sensing capabilities.

The control of dewetting behaviour to produce cellular patterns offers a potential templating system for preparation of large-scale microbial arrays that hold promise as platforms for BioMEMS devices, as diagnostic chips for detection of chemical pollutants and/or toxins in the environment (biosensing) and HTS applied to drug discovery.

References

[1] Klein R D and Geary T G 1997 Recombinant microorganisms as tools for high throughput screening for nonantibiotic compounds *J. Biomol. Screen.* **2** 41–9

[2] Broach J R and Thorner J 1996 High-throughput screening for drug discovery *Nature* **384** 14–6
Tucker C L 2002 High-throughput cell-based assays in yeast *Drug Discov. Today* **7** S125–30

[3] King K, Dohlman H G, Thorner J, Caron M G and Lefkowitz R J 1990 Control of yeast mating signal transduction by a mammalian b2-adrenergic receptor and Gsa subunit *Science* **250** 121–3
Price L A, Kajkowski E M, Hadcock J R, Ozenberger B A and Pausch M H 1995 Functional coupling of a mammalian somatostatin receptor to the yeast pheromone response pathway *Mol. Cell. Biol.* **15** 6188–95
Schena M and Yamamoto K R 1988 Mammalian glucocorticoid receptor derivatives enhance transcription in yeast *Science* **241** 965–7
Kralli A, Bohen S P and Yamamoto K R 1995 LEM1, an ATP-binding cassette transporter, selectively modulates the biological potency of steroid hormones *Proc. Natl Acad. Sci. USA* **92** 4701–5
Hall B L, Smit-McBride Z and Privalsky M L 1993 Reconstitution of the retinoid X receptor function and combinatorial regulation of other nuclear hormone receptors in the yeast *Saccharomyces cerevisiae Proc. Natl Acad. Sci. USA* **90** 6929–33

[4] Zhu H *et al* 2001 Global analysis of protein activities using proteome chips *Science* **293** 2101–5
Tong A H *et al* 2001 Systematic genetic analysis with ordered arrays of yeast deletion mutants *Science* **294** 2364–8

[5] Lee L T, Leite C A P and Galembeck F 2004 Controlled nanoparticle assembly by dewetting of charged polymer solutions *Langmuir* **20** 4430–5

[6] Lee L T, da Silva M D C V and Galembeck F 2003 Dewetting patterns of thin films of charged polymer solutions *Langmuir* **19** 6717–22

[7] Denkov N D, Velev O D, Kralchevsky P A, Ivanov I B, Yoshimura H and Nagayama K 1992 Mechanism of formation of two-dimensional crystals from latex particles on substrates *Langmuir* **8** 3183–90

[8] Satriano C, Carnazza S, Guglielmino S and Marletta G 2002 Differential cultured fibroblast behavior on plasma and ion beam-modified polysiloxane surfaces *Langmuir* **18** 9469–75

[9] Neumann A W and Good R J 1979 Techniques of measuring contact angles *Surface and Colloid Science* vol 11, ed R J Good and R R Stromberg (New York: Plenum) pp 31–91

[10] Carnazza S, Satriano C, Guglielmino S and Marletta G 2005 Fast exopolysaccharide secretion of *Pseudomonas aeruginosa* on polar polymer surfaces *J. Colloid Interface Sci.* **289** 386–93

[11] Ramsey A J 1978 Direct counts of bacteria by a modified acridine orange method in relation to their heterotrophic activity *N. Z. J. Mar. Freshwater Res.* **12** 265–9

[12] Marletta G and Iacona F 1995 Chemical and physical property modifications induced by ion irradiation in polymers *Materials and Processes for Surface and Interface Engineering* (*NATO Advanced Study Institute, Series E: Applied Sciences* vol 290) ed Y Pauleau (Dordrecht: Kluwer–Academic) pp 597–640

Marletta G and Satriano C 2004 Irradiation-controlled adsorption and organization of biomolecules on surfaces: from the nanometric to mesoscopic level *Frontiers in Multifunctional Integrated Nanosystems* (*NATO Science, Series II: Mathematics, Physics and Chemistry* vol 152) ed E Buzaneva and P Scharff Pauleau (Dordrecht: Kluwer–Academic) pp 71–94

[13] Satriano C, Carnazza S, Guglielmino S and Marletta G 2003 Surface free energy and cell attachment onto ion-beam irradiated polymer surfaces *Nucl. Instrum. Methods* B **208** 287–93

[14] Biran I, Rissin D M, Ron E Z and Walt D R 2003 Optical imaging fiber-based live bacterial cell array biosensor *Anal. Biochem.* **315** 106–13